ELSEVIER

Earth and Planetary Science Letters 166 (1999) 105–119

EPSL

# Climatic influence in NRM and $^{10}$Be-derived geomagnetic paleointensity data

Yvo S. Kok *

*Paleomagnetic Laboratory Fort Hoofddijk, Budapestlaan 17, 3584 CD Utrecht, Netherlands*

Received 16 August 1998; revised version received 7 January 1999; accepted 7 January 1999

**Abstract**

One can determine geomagnetic paleointensities from natural remanent magnetizations (NRM) and by inverting production rates of cosmogenic isotopes such as $^{10}$Be and $^{14}$C. Recently, two independently derived 200-kyr stacks [Y. Guyodo, J.-P. Valet, Relative variations in geomagnetic intensity from sedimentary records: the past 200,000 years, Earth Planet. Sci. Lett. 143 (1996) 23–36; M. Frank, B. Schwarz, S. Baumann, P.W. Kubik, M. Suter, A. Mangini, A 200 kyr record of cosmogenic radionuclide production rate and geomagnetic field intensity from $^{10}$Be in globally stacked deep-sea sediments, Earth Planet. Sci. Lett. 149 (1997) 121–129] were compared and the good agreement was suggested to validate the use of sedimentary cores for studies. Both compilations use mainly the astronomically forced and climatically controlled oxygen isotope stratigraphy to date and synchronize the sedimentary records, while this very curve has several coherent features with the supposedly pure geomagnetic records. An NRM relative paleointensity record, which was included in the conventional paleointensity stack, shows correspondence with climatic features, which is explained by an inadequacy in the normalization technique. Therefore, it is possible that the extraction of the pure paleointensity signal from marine sediments has not always been accomplished. 

*Keywords:* paleomagnetism; magnetic intensity; Be-10; climatic controls

## 1. Introduction

The records of variations of the paleomagnetic field of the Earth registered in rocks provide information on geophysical processes, for instance those related to the long-term history of its core. In general, lavas record most reliably information on the prevailing magnetic field by registering magnetic vectors during cooling. These spot-readings of absolute paleointensity have a more continuous equivalent in relative records reconstructed from sediments, which have proved to be able to register both directions and intensities of the ancient geomagnetic field (see review [1]). However, the mechanism of remanence acquisition is still not fully understood. Thus the translation of sedimentary magnetizations to geomagnetic information remains ambiguous. A recent compilation by Guyodo and Valet [2] of several globally distributed sedimentary records provides a coherent **S**ynthetic **int**ensity curve for the last 200 kyr (Sint-200). However, global agreement of variations in various sedimentary paleointensity records is a necessity, though not a sufficient proof that the

* E-mail: yvoskok@geo.uu.nl

0012-821X/99/$ – see front matter 
PII: S0012-821X(99)00006-0

evolution of the strength of the geomagnetic dipole field has been correctly recorded.

Many problems with sediments as recorders of geomagnetic field strength have been reported, e.g. by Kent [3]. He reminds us that Pleistocene NRM intensity records correlate well with lithological parameters driven by the same climatic forcing as $\delta^{18}O$ (oxygen isotopes) or carbonate content. It is likely that the intensity of NRM co-varies to some extent with climate change, but also has a component of the geomagnetic field strength. Normalization of such NRM intensities by magnetic susceptibilities $\chi$ or laboratory induced magnetizations gives relative paleointensity estimates. In principle, these normalized records should correlate negligibly with climatic features. However, if a normalized remanence record still correlates with for instance carbonate content, either some geomagnetic–climatic dependency or — more likely — an inadequacy in the normalization must exist [3]. Twenty years ago Wollin et al. [4] suggested a relationship between climate, intensity of the geomagnetic field and the eccentricity of the Earth's orbit. Somewhat later, Chave and Denham [5] and Kent [3] maintained that no connection is evident and that the previous results had been the consequence of a failure — or an omission — in removing the effect of a varying input of magnetic material, which is largely climatically controlled.

More recent studies cast additional doubt on the fidelity of sedimentary paleointensities. Schwartz et al. [6] suggest that about 25% of the low-frequency variation in their normalized paleointensity record can be biased by climatic or other environmental factors. The authors caution that extreme care must be taken to remove such influences from sedimentary paleointensity records, and they are concerned that other records are similarly affected. Worm [7] suggests a link between reversals, events, paleointensities and glaciations. According to him, the apparent correlations of normalized NRM intensity and $\delta^{18}O$ records are thought to stem from normalizing problems.

Not only time-domain records are tested, but also frequency analyses give interesting results regarding paleointensity data. Dominant periods between 30 and 40 kyr for relative paleointensity variations are found in records from the Ontong–Java Plateau, and are argued not to be an artifact of lithologic variability [8,9]. Some correspondence with periods describing the Earth's orbit appears, but those stacked records are too short for a meaningful discussion on geomagnetic–climatic dependency.

An independent estimate for geomagnetic field intensity variations is deduced from the recently published stack of cosmogenic beryllium-10 ($^{10}Be$) deposition rates for the last 200 kyr [10]. The normalized $^{10}Be$ stack is interpreted as a record of cosmogenic radionuclide production rates which are translated into relative geomagnetic field intensity changes (following [11]). These paleointensity variations correspond well with those from the conventionally determined paleointensity stack Sint-200 [2]. However, several studies hint that the local $^{10}Be$ deposition rates can be controlled by climatic factors, such as advection of different water masses on glacial–interglacial time scales [12], enhanced scavenging due to increased productivity [13], or increased glacial terrigenous particle flux [14]. Although the global stacking of records should average out these effects, one may fear that the translation from averaged $^{10}Be$ production rates to 100% variations of geomagnetic field intensity [10] is not always valid.

In this paper it will be shown that both recently published 200-kyr stacks, which mainly use the $\delta^{18}O$ chronology [15] to construct the age models, have coherent features with the oxygen isotope record itself. Different material and/or techniques are needed to obtain more reliable paleointensities from the sediments if persistent climatic contaminations are present in the geomagnetic signal. New data from an individual core, included in Sint-200, are presented to investigate whether more sophisticated normalization techniques can reduce the coherence with environmental factors.

## 2. Stacks for the last 200 kyr

Shown in Fig. 1 are the stacked profiles of sedimentary records for oxygen isotopes [15] ($\delta^{18}O$), conventional NRM paleointensities [2] (Sint-200), and the expected geomagnetic field intensities derived from $^{10}Be$ deposition rates [10] (for brevity I will refer to this **S**ynthetic geomagnetic **int**ensity stack as Sint-Be). The $\delta^{18}O$ record has a very smooth

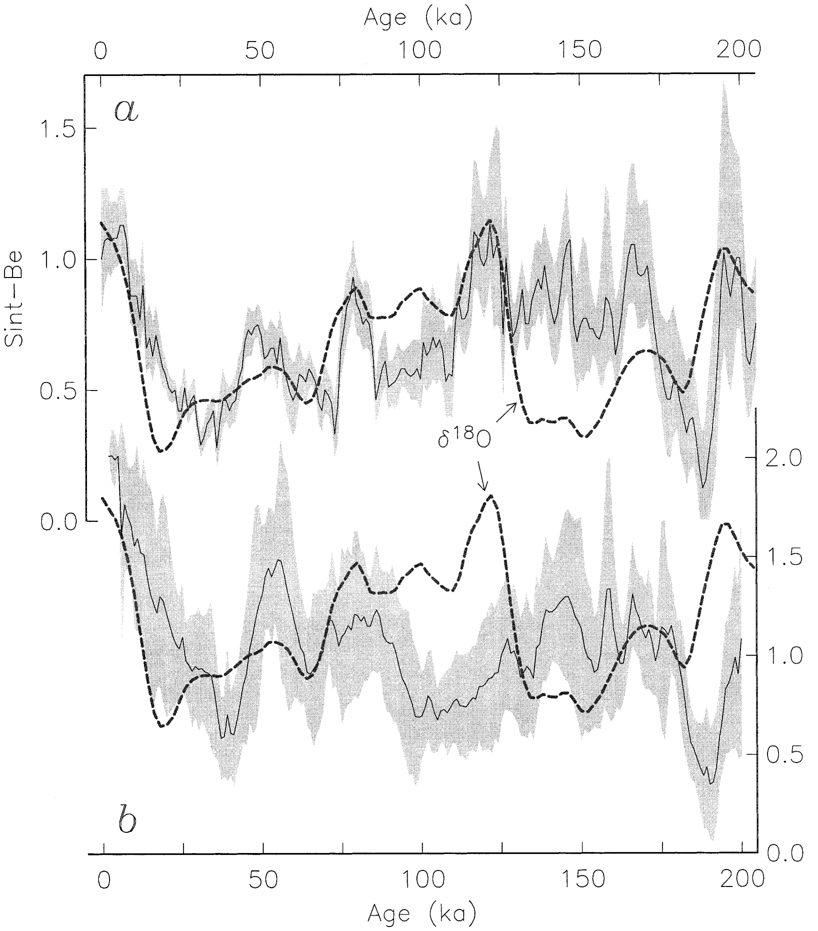


Fig. 1. Independent paleointensity records for the last 200 kyr with error estimates (gray) and the $\delta^{18}$O curve (dashed) representing global climate variability. (a) Stack of $^{10}$Be production rates inverted to geomagnetic field strength [10]. (b) Stack of relative paleointensities determined the conventional way [2]. Fluctuations in both (a) and (b) are compared to the oxygen isotope signature.

('over-stacked') character and conforms to the convention depicting 'warm climate' (small global ice volume) up and 'cold climate' (large global ice volume) down.

Frank et al. [10] point out the impressive agreement between Sint-Be (Fig. 1a) and Sint-200 (Fig. 1b). However, upon close inspection, it is noticeable that a slight shift of Sint-200 to younger ages would improve the fit. More importantly, the $\delta^{18}$O curve contains many features that are present in both relative paleointensity records. In particular, the strong correspondence between $\delta^{18}$O and Sint-Be seems to contradict the assumption of Frank et al. [10] that climatic influences are averaged out in the $^{10}$Be compilation, even though the agreement is not as evident in the 160–130 ka interval (Fig. 1a). One must keep in mind that non-geomagnetic factors have influenced the beryllium records as well, and that it is assumed that for the *entire* 200-kyr period no link between paleomagnetic field strength and $\delta^{18}$O exists. Comparing the $^{10}$Be-based record to Sint-200, an inconsistency in the 125–115 ka interval is mentioned [10] which corresponds extremely well to oxygen isotope stage 5.5 ($\sim$120 ka). Frank et al. [10] argue that, by coincidence, this may have been an interval with uniformly reduced local $^{10}$Be rain rates. It is also possible that this interval is hampered by a number of sediment cores with relatively high

$^{230}Th_{ex}$ concentrations that are used to normalize the $^{10}Be$ data [16].

### 2.1. Cross-spectral analysis

To further investigate the correspondence between two time series, one can calculate correlation coefficients, however, their significances strongly depend on the amount of data. The data also need to be Gauss-Laplace distributed, which is not always the case and is rarely checked for paleointensity data. A more quantitative means to determine the degree of resemblance of two data sets is cross-analysis of spectral power. This technique, first described for paleointensity data by Tauxe and Wu [8], and more recently by Constable et al. [17] (whose code is used in this manuscript), can reveal potentially important relationships. The squared coherence $\gamma^2$ of two uncorrelated Gauss-Laplace distributed time series are expected to fall below a so-called zero-coherence level 95% of the time. Constable et al. [17] recommend that the phase spectrum of $\gamma^2$ should be used as an additional diagnostic.

Frequency analyses of the Earth's paleoclimate or $\delta^{18}O$ records exhibits the Milankovitch periods of ca. 100 kyr for eccentricity, 41 kyr for obliquity, and 23 and 19 kyr for precession (see e.g. [15]). Both paleointensity data sets have power spectrum density (PSD) concentrations at and near the orbital frequencies as well (Fig. 2a). Fig. 2b shows the squared coherence as function of frequency for the three curves. When $\gamma^2$ is higher than the zero-coherence level of ca. 0.21, frequencies are considered significantly coherent. Although the coherences between the conventional Sint-200 paleointensity stack [2] and the beryllium based Sint-Be stack [10] (Sint-200 and Sint-Be) are clearly the most prominent, significant coherences at or near some of the Milankovitch frequencies are present for the other combinations as well. The phase diagrams for the coherence of all combinations (Fig. 2c) suggest that all records are not in phase with each other, but that small and rather consistent delays are present. The 100-kyr component lacks in Sint-Be and $\delta^{18}O$ (and Sint-200 and Sint-Be), but this eccentricity component should be ignored because the records are only twice its cycle length. Also the phase diagram indicates non-uniform behavior in the left part of the spectrum (i.e., in the interval 0.00–0.02 kyr$^{-1}$). Furthermore, the 41-kyr component is missing in Sint-200 and $\delta^{18}O$, but present in $^{10}Be$ and $\delta^{18}O$, whereas Fig. 2a suggests that the paleointensity curves have rather similar power spectral density. Moreover, the Nyquist frequency of the paleointensity records with 1-kyr data spacing would be 0.5 kyr$^{-1}$, but Guyodo and Valet [2] warn that variations shorter than 5 kyr cannot be extracted from their record, since the sample frequency of the original records in Sint-200 much lower than 1 per kyr. Therefore, frequencies higher than ca. 0.08 kyr$^{-1}$ are not meaningful, also because the phase data become unstable. Furthermore, all the positions of the peaks discussed here might be slightly out of tune because of the frequency resolution of the data. Although the peaks in PSD (Fig. 2a) are insignificant in comparison with the calculated error bars, it is plausible that such peaks at or near orbital frequencies should reflect the climate's control in the records (see also [17]).

The above mentioned problems illustrate the limitations of squared coherence analysis on these rather short stacked records. Still, the benefits of working in the frequency domain, rather than a correlation coefficient of the time series, are clear. Just for the record, the correlation coefficient for the two Sint records is 0.492, for Sint-Be and $\delta^{18}O$ 0.298, and for Sint-200 and $\delta^{18}O$ 0.079. One should consider that the 5% and 1% significance levels for 198 degrees of freedom are respectively 0.138 and 0.181, which would imply that Sint-Be and $\delta^{18}O$ are well correlated, but not Sint-200 and $\delta^{18}O$.

## 3. Individual record

Compilations that include a number of globally distributed records from different environments will not perfectly represent the behavior of magnetic paleointensity or $\delta^{18}O$. In the previous section, exact one-to-one matches between the records of magnetics and climate may be obscured. Consequently, one turns to a high-resolution record that has detailed oxygen isotope and paleomagnetic data. The piston core SU-92-18 from the Azores area published by Lehman et al. [18], which has a sedimentation rate ca. 3.6 cm/kyr, is selected from the Sint-200 stack because it is one of the few records that span the

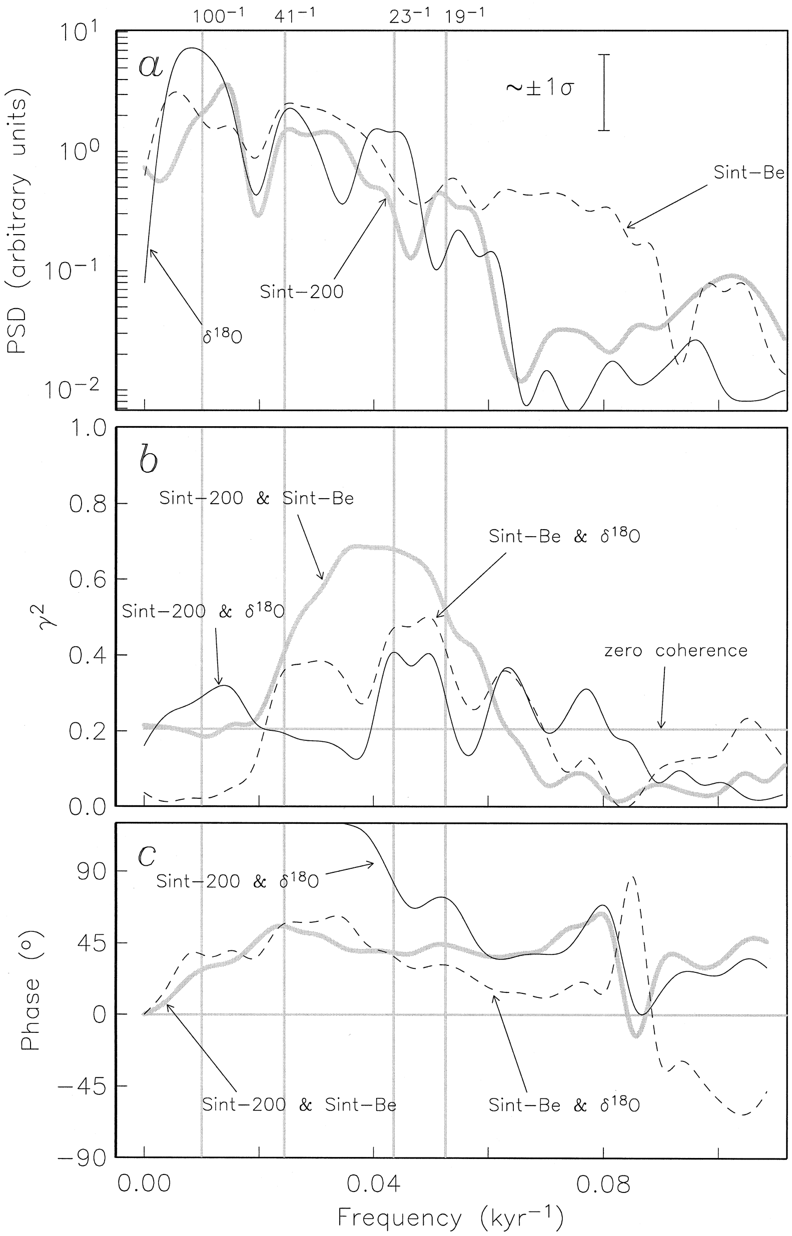


Fig. 2. Spectral analysis results for the three stacks of the previous figure. (a) All records contain power spectrum density (*PSD*) at Milankovitch frequencies. (b) Squared coherences $\gamma^2$ above zero-coherence are significant (95% confidence level) at several frequencies. The resemblance of Sint-200 and Sint-Be is most prominent, though other combinations show cross-spectral coherence as well. Note that the $\delta^{18}O$ stack contains relatively little power at the frequencies where $\gamma^2$ peaks in Sint-200 and Sint-Be. (c) Phase of squared coherences of (b)

entire interval of 200 kyr. It appears that the NRM (demagnetized to 25 mT) agrees well with the $\delta^{18}O$ of this core (Fig. 3a), and it is therefore corrected by an estimate of 'magnetizability': anhysteretic remanent magnetization (ARM). Note that the upper axes of the magnetizations are shifted 5 kyr ($\approx$18 cm) to younger ages with respect to the lower ones of oxygen isotopes to improve the fit (see later discussion).

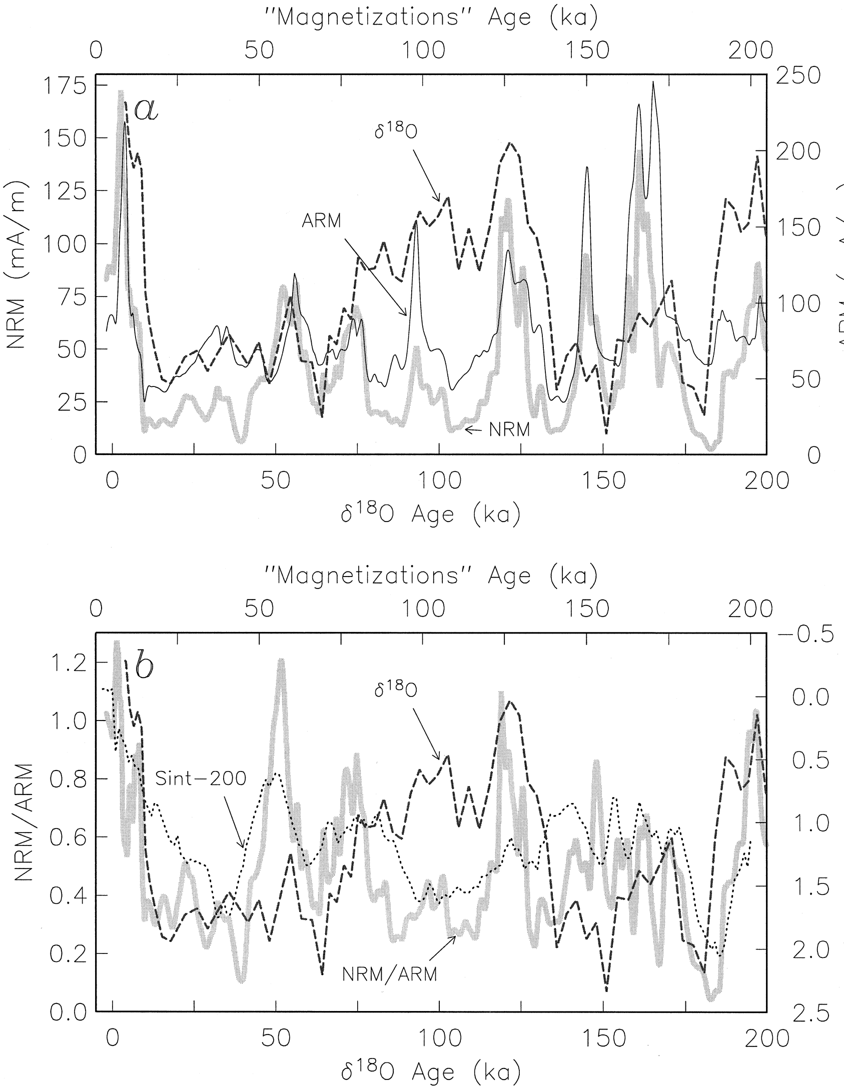


Fig. 3. (a) NRM intensity of core SU-92-18 [18] (gray) depicts strong correlations with the oxygen isotopes (dashed), the normalizer ARM (black) is concordant. Both remanences have been demagnetized at 25 mT. (b) The NRM/ARM ratio (gray) contains several features that correlate with the $\delta^{18}O$ curve (dashed); in other words, this relative paleointensity estimate does not seem to be sufficiently free of climatic influences. Note the 5-kyr shift of the magnetizations to 'younger ages' (upper axes). Sint-200 (dotted) shows good correlation with NRM/ARM, but often misses the specific signatures of the $\delta^{18}O$ curve of this core.

The correspondence between the ratio NRM/ARM (Fig. 3b) and the oxygen isotopes for this individual core is more evident than the one between the stacks Sint-200 and $\delta^{18}O$ (Fig. 1b). In this Atlantic record, characteristic signatures in paleointensity often correlate with variations in the oxygen isotope curve, in spite of the normalization. Examples are the paleointensity high at ~125 ka (isotopic stage 5.5), the low at ~180 ka (isotopic stage 6.6), and, despite the offset in amplitude, the pattern from ca. 115 to 80 ka can be matched to isotopic stages 5.4–5.2. When compared to the Sint-200 curve (dotted in Fig. 3b), the NRM/ARM paleointensity estimate has similarities, but interesting discrepancies as well, for instance, a usual characteristic for stacks like Sint-200 is that high-amplitude and high-frequency features are filtered. Non-dipole contributions in the individual record, which are likely to have been averaged out in the stack, can also cause differences. Core SU-92-18 has a 'rather high' coefficient of correlation with Sint-200 (0.64 in [2]).

### 3.1. Thellier-Thellier paleointensity estimates

Because there is reason to suspect that the NRM/ARM ratio is not a perfect determination of the paleointensity, the core has been resampled and discrete samples were subjected to different paleointensity methods. Thermal methods have been performed on part of the resampled collection. This took place in the shielded room of Scripps Institution of Oceanography, in an identical manner to that used in earlier encouraging studies on deep-sea sediments [19,20]. Although thermal paleointensity techniques on sediments are increasingly used, the mechanism of detrital remanent magnetization (DRM) is fundamentally different from thermoremanent origin. Therefore, absolute paleointensity estimates will be difficult to obtain from sediments, whereas volcanics do give rise to absolute values. An example of sedimentary Thellier-Thellier experiment is shown in Fig. 4 for a sample with age 77 ka. The NRM demagnetization shows a gradual decrease of the magnetic vector. The pTRM acquisition shows a very typical change after 275ºC, which might be explained by alteration from magnetite to maghemite caused by repetitive heating. Thermomagnetic runs on these sediments suggest that after temperatures as high as 325–350ºC the magnetic phases slightly change. In any case, the Arai plot (Fig. 4c), which ties NRM to corresponding pTRM, can only be used up to 275ºC. For this example, the best-fit slope through at least 3 data points is $-0.056$, which is found between 175–250ºC.

Crucial information about the uncertainty in the best-fit line is obtained by a jackknife method (Kok et al., in prep.). On all samples, jackknife resampling of the NRM–TRM pairs in the interval 150–275ºC is performed to obtain additional estimates for the best-fit slope. The central 90% of the distribution of 21 extra paleointensity estimates comprises the original slope and steeper slopes up to $-0.073$ (see Fig. 4d). This error indication is not symmetrically distributed around the best-fit slope, contrary to a standard deviation. Fig. 5a depicts the best-fit slopes picked between 150 and 275ºC (filled circles) and jackknife error estimates as a gray band. These thermal data could suggest a rather constant paleointensity pattern for the last 200 kyr, with a distinct decrease in paleointensity between ca. 190 and 180 ka. However, the amount of samples is small and it is likely that aliasing has occurred.

The absolute paleointensity data set has recently been extended with a record from Hawaiian lava flows, and has been compared with the sedimentary stack Sint-200 by Brassart et al. [21]. The two records are not inconsistent, but an alternative interpretation of the virtual axial dipole moments (VADM) of the 8 lava flows (ca. 400–60 ka) is that the paleointensity has varied less than sedimentary records suggest. Fig. 5a also includes the new results [21] (symbols with error bars) for the last 200 kyr, and the fit with the new thermal paleointensities of SU-92-18 is acceptable.

### 3.2. Pseudo-Thellier paleointensity estimates

A pseudo-Thellier approach [23] on the resampled collection of SU-92-18 sediments shows, to first order, similar results as the NRM/ARM paleointensity estimates [22]. Fig. 5b indicates pseudo-Thellier slopes $m_a$ (dashed line) and corresponding jackknife uncertainty bounds (gray). The trend of this pseudo-Thellier record is similar to the one of the Thellier-Thellier data (Fig. 5a vs. b). One could argue that the paleointensities have been more stable than the alternating field results of Fig. 3b (and Fig. 5b) indicate, but the thermal results of SU-92-18 can be hampered by under-sampling (Fig. 3a). As already mentioned in [21], the possibly too broad intensity low from sediments in 190–175 ka in Sint-200, but also all three records of SU-92-18, could be caused by other factors than the geomagnetic field behavior.

### 3.3. Cross-spectral analysis

Since there now is different data from one single core, we can perform more detailed and more appropriate squared coherences tests. Although in the interval 0–200 ka the thermally derived sedimentary paleointensity estimates outnumber the absolute paleointensity determinations of Brassart et al. [21],

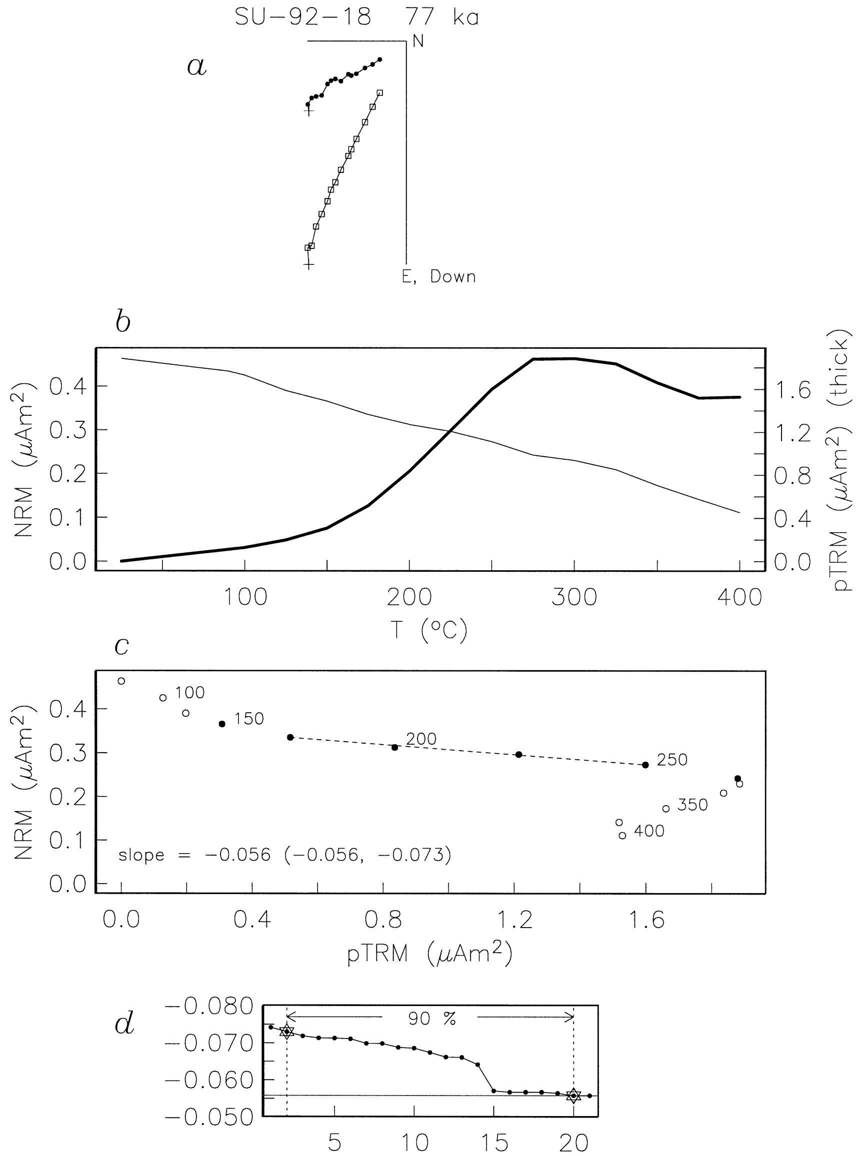


Fig. 4. An example of Thellier-Thellier paleointensity determination on sediment of SU-92-18. (a) Zijderveld diagram depicts step-wise destruction of the net magnetic moment. (b) NRM intensity gradually decays on higher temperature steps. Peculiar behavior in the pTRM acquisition is observed after 275ºC. This temperature step is therefore the highest to be used in the Arai plot (c). A relative estimate for the geomagnetic paleointensity is given by the slope determined between 175 and 250ºC. (d) Representation of the 21 additional jackknife slopes in ranked order. The central 90% excludes the two most extreme data.

their sample density is still far too low to be used in frequency analyses. Just the pseudo-Thellier slopes $m_a$, NRM, ARM, their ratio, and $\delta^{18}O$ of SU-92-18 are tested against each other and against Sint-200.

The zero-coherence level for the analysis of this core is now ca. 0.31 because of the smaller amount of data, as compared to the number of data points in the Sint-stacks. First of all, NRM/ARM corresponds fairly well to Sint-200 (Figs. 3 and 6a), and the routine check whether NRM/ARM is coherent with ARM indicates slight coherence, for example at 0.035 $kyr^{-1}$. More importantly, NRM/ARM with

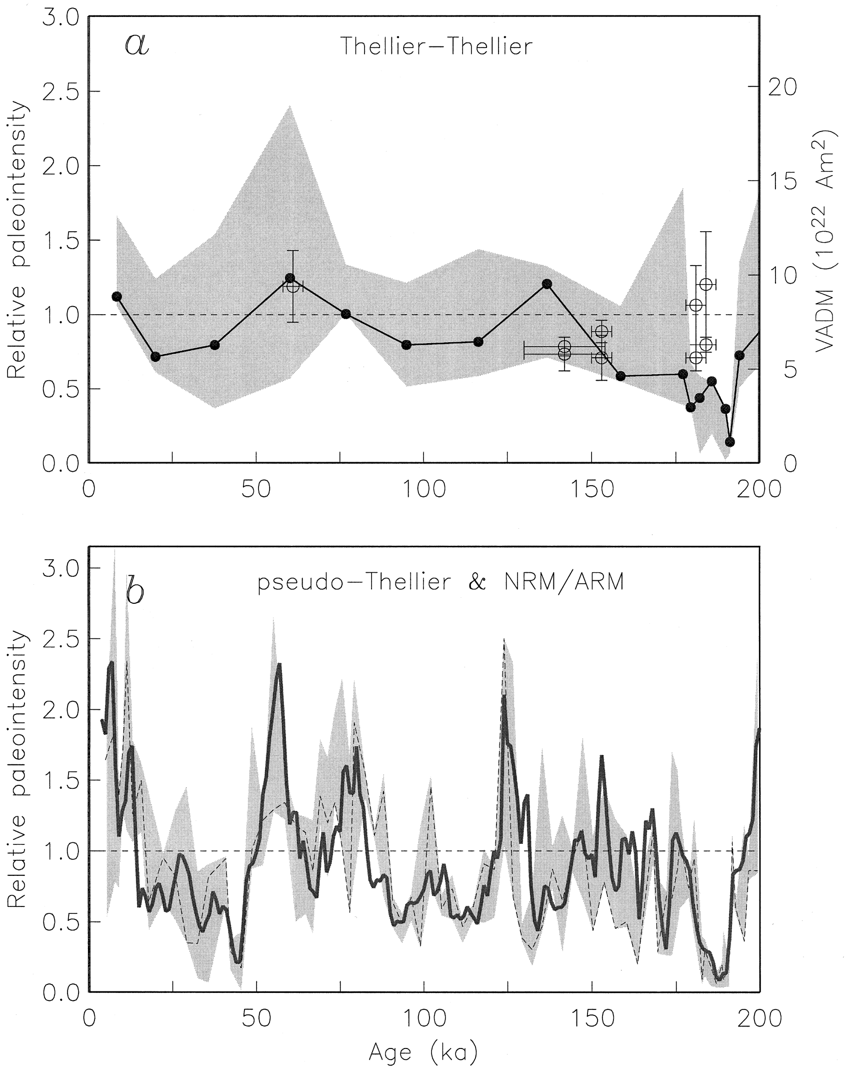


Fig. 5. Paleointensity estimates as function of age for SU-92-18. (a) Best-fit slope results from Thellier-Thellier for sediments indicated by filled circles with their jackknife error estimate in gray, show a rather constant paleointensity behavior for the last 175 kyr. Absolute determinations in VADMs (open symbols) from a recent study by Brassart et al. [21] do not contradict the sedimentary data. The horizontal dashed line indicates the present-day dipole moment of $8 \times 10^{22}$ A m$^2$. (b) Pseudo-Thellier results of this core (dashed curve) and jackknife error bounds (gray) [22], thick line represents the original NRM/ARM data [18]. In principle, the data are similar though subtle differences are present. The horizontal dashed line indicates the mean of the record.

$\delta^{18}$O gives squared coherences above zero coherence at precessional frequencies, leading to suspect a slight but significant climatic influence. The middle panel shows that NRM and ARM are similar (Fig. 6b), as already noted from Fig. 3b. These remanent magnetizations have common features with the oxygen isotopes near the precession frequency band (ca. 0.03–0.05 kyr$^{-1}$). Ideally, a proper normalization of NRM by ARM should eliminate all environmental influences, but apparently this is not the case. Finally, the paleointensity slope $m_a$ is subjected to the coherence check (Fig. 6c). The strong coherence between $m_a$ and the faster NRM/ARM method [18] is evident, although a dip can be recognized in the precession interval. Also, Sint-200 and $m_a$ correlate fairly well over a rather broad frequency

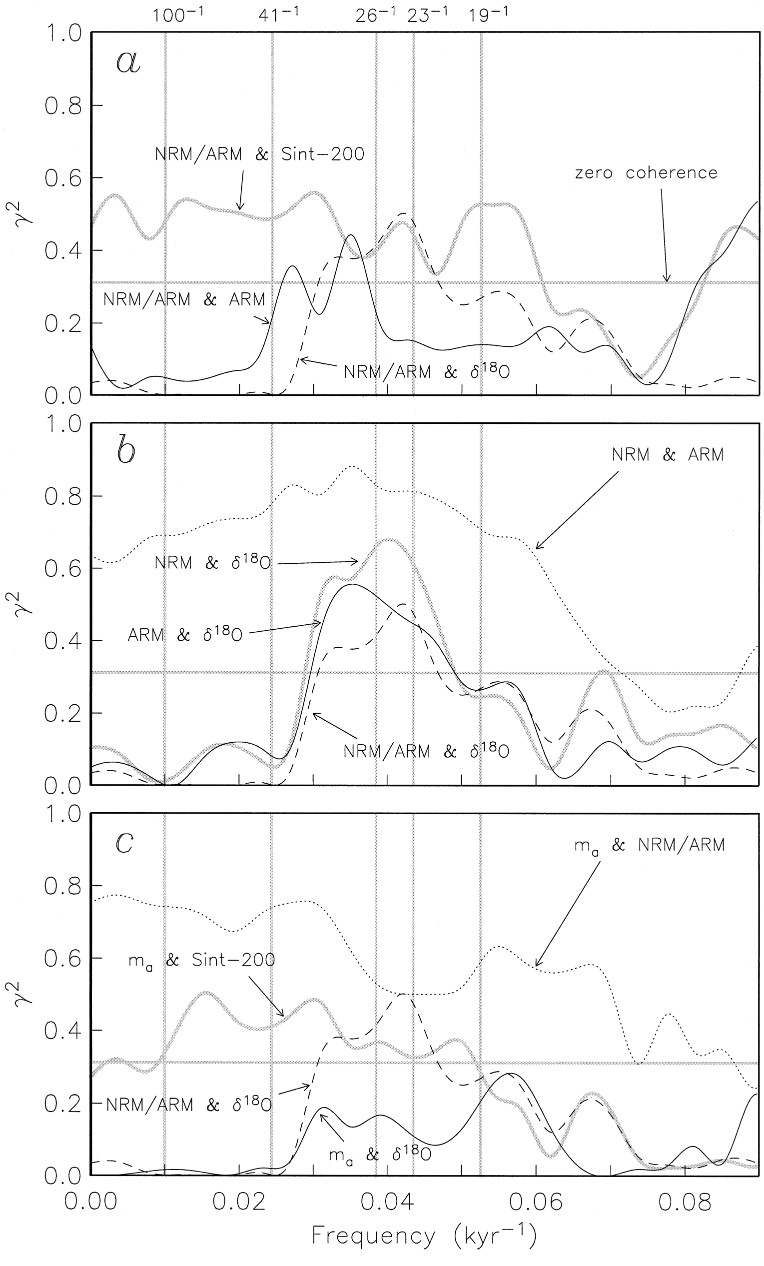


Fig. 6. Squared coherence tests for SU-92-18. (a) The paleointensity estimate NRM/ARM is coherent with Sint-200 (which includes the Azores core). The test whether ARM did a fair job in normalizing the NRM (i.e., NRM/ARM and ARM) shows slight coherence; it is less pronounced than the coherence of NRM/ARM and $\delta^{18}O$. (b) The NRM and ARM are highly coherent, which could eventually validate the use of ARM as a normalizer. Both NRM and ARM have coherent features with oxygen isotopes, and also their ratio NRM/ARM is above the zero-coherence level. (c) The pseudo-Thellier slope $m_a$ is coherent with the original paleointensity determination, though a dip is observed at the precession frequencies. The squared coherence of $m_a$ with $\delta^{18}O$ has dropped below the zero-coherence level, suggesting that $m_a$ has lost the climatic contamination that conflicted with the geomagnetic character in NRM/ARM.

interval. However, where NRM/ARM and $\delta^{18}O$ cohere, the more elaborate paleointensity determination seems to have lost its resemblance with oxygen isotopes. The pseudo-Thellier approach is designed to suppress climate influences [23], in contrast to NRM/ARM which appears to contain some climatic contamination. However, one should take care in interpreting the $\gamma^2$ plots. Possibly, the squared coherences of $m_a$ and NRM/ARM with $\delta^{18}O$ are too close to the zero-coherence level to be distinguished as significantly coherent. Also, deviating data in either record can strongly influence the spectral power. Furthermore, the records have been interpolated and are possibly too short and not densely enough sampled for frequency purposes. Finally, in 5% of the cases the squared coherence exceeds zero coherence from chance. Most probably, the 'safe' conclusion to be drawn is that the records NRM, ARM, and their ratio cohere with $\delta^{18}O$. Consequently, a stack of more or less comparable records (like Sint-200) is likely to contain climate influences.

## 4. Ineffective normalization

As a first order approximation, the natural remanent magnetization (NRM) depends on the paleomagnetic field and a response function of the sediment:

$$\mathrm{NRM}(X,t) = M(t) \times f(X,t) \tag{1}$$

with $M(t)$ as the desired true field behavior of the geomagnetic intensity as a function of age $t$. The non-linear function $f$ depends on many variable factors, such as grain size, carbonate content, sedimentation rate, bioturbation, diagenesis, all driven by environmental conditions. Its arbitrary parameter $X$ represents climate, which is perhaps best approximated by the data of $\delta^{18}O$ [15] and to a lesser extent by, for instance, magnetic susceptibility $\chi$. The sediment function $f$ is usually approximated by bulk magnetic parameters or laboratory induced magnetizations, such as anhysteretic remanence (ARM), that is:

$$\mathrm{ARM}(X,t) = g(X,t) \approx f(X,t) \tag{2}$$

Normalization of NRM by ARM will give a relative paleointensity estimate:

$$\frac{\mathrm{NRM}(X,t)}{\mathrm{ARM}(X,t)} = M(t) \times \frac{f(X,t)}{g(X,t)} \tag{3}$$

Only if $g(X,t)$ is linearly related to $f(X,t)$, the ratio of Eq. 3 is proportional to the true field behavior $M(t)$, and consequently a relative paleointensity independent of $X$ is accomplished. From Fig. 3 it is obvious that the ratio NRM/ARM corresponds in a number of cases to the sedimentary response function $\delta^{18}O(X,t)$; the most 'pure' function of $X$, which is independent of magnetic field strength. Also the squared coherence $\gamma^2$ (Fig. 6) suggests involvement of climate $X$ in the paleointensity curve NRM/ARM.

Oftentimes, other normalizers of NRM, such as $\chi$ or IRM, yield very consistent paleointensity estimates within a particular core. It is likely that these responses are again not linearly related to the complex $f(X,t)$ in Eq. 1, but are comparable to $g(X,t)$ of ARM in Eq. 2. Stacking several records like SU-92-18 will give a more or less coherent estimate for $M(t)$. Its reliability in representing solely the geomagnetic paleointensities must be questioned when correlations with purely environmental functions like $\delta^{18}O$ are still evident.

## 5. Discussion

### 5.1. Climatic influence in beryllium data

Is it possible that the stacked $^{10}Be$ deposition rates from marine sediments are contaminated by a climatic signal? There are several studies on $^{10}Be$ data that indicate climatic involvement.

First of all, it is well known that there is a climatic influence or control on the $^{10}Be/^{230}Th_{ex}$ ratio in marine sediments [13,14,24]. Increased values during glacial periods are even used as a proxy for paleo-particle flux on glacial–interglacial time scales and may be attributed to enhanced scavenging intensity. Strong climatic controls are found in high-resolution profiles of $^{230}Th_{ex}$ and $^{10}Be$ from the southernmost Atlantic Ocean (Weddell Sea), that deliver a stratigraphy similar to the $\delta^{18}O$ variations [25]. These records are not included in the present $^{10}Be$-stack [10] because of their variable contributions of old, rapidly resedimented particles and changes in bottom-water currents on interglacial–glacial time scales. This very local phenomenon of the Antarctic continental margin is not representative for the variable advection in the entire Atlantic ocean, still a direct link with climate is evident.

Second, in a study on Fe–Mn crusts [12], it is suggested that fluctuations in $^{9}$Be-normalized records of $^{10}$Be might be caused by variations in the Atlantic-Ocean circulation. The change in the global thermohaline conveyor pattern could well effect the distribution of dissolved $^{10}$Be/$^{9}$Be in the deep sea. However, the $^{10}$Be stack [10] incorporates only accumulation rates normalized by $^{230}Th_{ex}$. This is done to obtain $^{10}$Be deposition rates primarily influenced by boundary scavenging effects and production rate variations.

Third, a $^{10}$Be study on the youngest 80 kyr of SU-92-18 [26] shows that approximately half of the variability of the $^{10}$Be/$^{9}$Be ratio can be explained by variations in the global geomagnetic intensity as inferred from NRM/ARM. The authors argue that the remaining differences could be caused by uncertainties in the assumed relationship or inaccuracies in either record. Instead of resulting from a change in cosmic-ray intensity through variation of the paleomagnetic field strength [26], the $^{10}$Be/$^{9}$Be increase in this core during the last glacial maximum might also be explained by a changed import of Antarctic Bottom Water [12]. However, it should be noted that the $^{10}$Be/$^{9}$Be ratios in this study are an order of magnitude lower than data for authigenic deposits, which could result in the observed discrepancies.

Finally, it is argued in Ref. [10] that although the major part of the long $^{10}$Be records cluster in the Southern Atlantic Ocean, the equal distribution north and south of the Polar Front averages out drastically different paleoflux conditions. Consequently, the $^{10}$Be stack is suggested to represent a global signal. However, the global distribution of the (long) $^{10}$Be cores used is rather uneven (see fig. 2 in [10]), which may result in incorrect averaging of local effects. This approach can give systematic errors in the Sint-Be stack. Whereas the global $^{10}$Be deposition rate as function of time could in fact be controlled for 100% by paleomagnetic intensity, the transport of the cosmogenic isotopes to specific areas and the accumulation in ocean sediments is to a significant extent driven by paleoclimatic controls.

Thus, there is evidence that beryllium-10 records in the Atlantic Ocean are not only affected by the geomagnetic field strength, but also by changes induced by global climate. It is difficult to unambiguously link circulation in the Atlantic Ocean and/or other glacial–interglacial phenomena to changes in the $^{10}$Be stack. Moreover, it is beyond the compass of the present study to solve this debate. Merely the observation that Sint-Be acts as $\delta^{18}$O, together with (indirect) evidence that $^{10}$Be is influenced by climate, makes the assumption that the entire $^{10}$Be stack is not influenced by ocean circulation variations or glacial–interglacial successions of Frank et al. [10] seem too optimistic.

### *5.2. Climatic influence in NRM paleointensity data*

The correspondences between the $\delta^{18}$O record and the conventionally determined Sint-200 may also be attributed to the sedimentary response to climate. Certainly, amplitude variations in the magnetic intensity have occurred in the past, but the traditional normalization for obtaining relative paleointensity behavior from natural remanences apparently fails to eliminate all climatic influences. The compilation Sint-200 [2] cannot be used in a one-to-one case versus the $\delta^{18}$O curve [15], therefore, an individual high-resolution record with detailed oxygen isotope and paleomagnetic data is subjected to the squared coherence test. Core SU-92-18 suggests that both sedimentary magnetization NRM and rock-magnetic parameter ARM have reacted to environmental features. Their ratio implies that pure geomagnetic paleointensity is not achieved through this normalization procedure (Figs. 3 and 6). Other paleointensity techniques suggest to provide better estimates with respect to climatic influence. The pseudo-Thellier approach [23] for sedimentary paleointensity data (see also [22]) shows subtle differences with the standard normalization methods. It causes the squared coherences near precessional frequencies to drop below the zero-coherence level. This is interpreted as a more correct approach to reconstruct estimates from sediments.

Instead of a delayed acquisition of magnetization, the phase shift between the magnetizations and $\delta^{18}$O (Fig. 2c and the shift of axes in Fig. 3) can be explained by the shift of a few thousand years between carbonate content and $\delta^{18}O$ [27]. Magnetite concentration in the North Atlantic is in phase with carbonate content, therefore a comparable delay between NRM (or ARM) and $\delta^{18}O$ can be expected.

### 5.3. Pure geomagnetic signal

The youngest ca. 50 kyr indicate a discrepancy between $\delta^{18}O$ and the paleointensity stacks (Fig. 1). The last glacial maximum is some 15 kyr younger than the minimum in magnetic intensity, which seems to be too large a shift for the above-mentioned lag [27]. In addition, this interval is most densely covered with normalized $^{10}Be$ and NRM data, so we may assume a more accurately determined geomagnetic character. Moreover, both paleointensity stacks coincide very well with the U/Th calibration results of the $^{14}C$ time scale [28–30]. Whereas the paleointensity low at ca. 40 ka does not coincide with a glacial maximum, the rest of the paleointensity trend in this youngest part is quite similar to climatic behavior, not only for the stacks, but also SU-92-18 (Fig. 3b). This could suggest that only anomalous geomagnetic intensity happened around 35–40 ka and the practically monotonously increasing values since are climatic artifacts. Independent support for this contention is given by the relative data from Site 983 which do not indicate an increasing trend for the last 35 kyr [31].

With respect to the cross-spectral analyses of the entire stacks, the highest coherence between Sint-200 and Sint-Be (Fig. 2b) favors the assumption that both have indeed been mainly controlled by the then prevailing magnetic fields. The agreement confirms the concentration of periodicities in the Brunhes paleointensity data in the ~33 kyr band [8,9]. However, the $\delta^{18}O$ stack does not contain much spectral power between obliquity and precession ($41^{-1}$ and $\sim 23^{-1}$ respectively), therefore coherences with both paleointensity stacks are bound to be low in this interval.

In a recent study Channell et al. [32] suggest that the obliquity power is a property of the geomagnetic field itself. The NRM/IRM against IRM data suggest insignificant coherence at the interval around obliquity, whereas at other orbital frequencies the normalization by IRM has failed to suppress lithological variations [32]. However, the absence of a 41-kyr peak in the power spectrum of the IRM data is noteworthy since the other possible normalizers ARM and susceptibility have roughly twice as much normalized power at the obliquity-related frequency. It might be that IRM is not the ideal normalizer of NRM and that these sedimentary records are lithologically contaminated to a larger extent than Channell et al. [32] suggest. Therefore, before hypotheses on orbital influence on the geomagnetic field can be tested with relative paleointensity records from sedimentary data, one must be certain that all sedimentary artifacts are accounted for.

## 6. Conclusion

The Sint-200 stack of several relative paleomagnetic intensity records for the last 200,000 years undoubtedly demonstrates an overall internal coherence. Independent support, from inverting the stacked $^{10}Be$ record to 100% paleofield intensity fluctuations, has been taken as a validation of the applicability of sediments for paleointensity research. Alternatively, I suggest that the good agreement of the stacked paleointensity records stems — to a certain extent — from similar influences of Pleistocene climate, rather than from geomagnetic intensity variations alone.

A detailed look at a conventionally determined paleointensity record suggests that even after normalization of the natural remanent magnetizations, the magnetic signals resemble the climatically controlled $\delta^{18}O$ records from the same core. Such ‘impure’ paleointensity records, which contain climatic components, are likely to result in coherent stack. Other more time-consuming relative paleointensity estimates seem to do a better job in removing the climatic influence.

Whereas it is not proved that fluctuations in the sedimentary paleointensity records are in fact affected by variations in global climate as opposed to being of geomagnetic origin, there are certainly grounds for suspicion.

## Acknowledgements

I am grateful to Martin Frank for kindly providing previews of manuscript and data, and the constructive reviews. Also many thanks to the Gif-sur-Yvette group and Pauline Kruiver for resampling core SU-92-18 and access to their data. Bob Parker is thanked for the cross-spectral analysis code, and the Keck Foundation for providing funds for the Scripps paleomagnetic laboratory. The manuscript has been improved by Harmen Bijwaard, Cor Langereis, Lisa Tauxe, and referees. Fruitful discussions with Michael Urbat, Teresa Juárez, Jaume Dinarès-Turell were enjoyable. The investigations are supported by the Netherlands Geosciences Foundation (GOA) with financial aid from the Netherlands Organization for Scientific Research (NWO) (750.194.09). ***[RV]***

## References

[1] L. Tauxe, Sedimentary records of relative paleointensity of the geomagnetic field in sediments: theory and practice, Rev. Geophys. 31 (1993) 319–354.

[2] Y. Guyodo, J.-P. Valet, Relative variations in geomagnetic intensity from sedimentary records: the past 200,000 years, Earth Planet. Sci. Lett. 143 (1996) 23–36.

[3] D.V. Kent, Apparent correlation of paleomagnetic intensity and climatic records in deep-sea sediments, Nature 299 (1982) 538–539.

[4] G. Wollin, W.B.F. Ryan, D.B. Ericson, Climatic changes, magnetic intensity variations and fluctuations of the eccentricity of the Earth's orbit during the past 2,000,000 years and a mechanism which may be responsible for the relationship, Earth Planet. Sci. Lett. 41 (1978) 395–397.

[5] A.D. Chave, C.R. Denham, Climatic changes, magnetic intensity variations and fluctuations of the eccentricity of the Earth's orbit during the past 2,000,000 years and a mechanism which may be responsible for the relationship — a discussion, Earth Planet. Sci. Lett. 44 (1979) 150–152.

[6] M. Schwartz, S.P. Lund, T.C. Johnson, Environmental factors as complicating influences in the recovery of the quantitative geomagnetic-field paleointensity estimates from sediments, Geophys. Res. Lett. 23 (1996) 2693–2996.

[7] H.-U. Worm, A link between geomagnetic reversals and events and glaciations, Earth Planet. Sci. Lett. 147 (1997) 55–67.

[8] L. Tauxe, G. Wu, Normalized remanence in sediments of the Western Equatorial Pacific: Relative paleointensity of the geomagnetic field?, J. Geophys. Res. 95 (1990) 12337–12350.

[9] L. Tauxe, N.J. Shackleton, Relative paleointensity records from the Ontong-Java Plateau, Geophys. J. Int. 117 (1994) 769–782.

[10] M. Frank, B. Schwarz, S. Baumann, P.W. Kubik, M. Suter, A. Mangini, A 200 kyr record of cosmogenic radionuclide production rate and geomagnetic field intensity from $^{10}$Be in globally stacked deep-sea sediments, Earth Planet. Sci. Lett. 149 (1997) 121–129.

[11] D. Lal, Theoretically expected variations in the terrestrial cosmic-ray production rates of isotopes, Soc. Ital. Fis. Bologna 95 (1988) 216–233.

[12] F. Von Blanckenburg, R.K. O'Nions, N.S. Belshaw, A. Gibb, J.R. Hein, Global distribution of beryllium isotopes in deep ocean water as derived from Fe–Mn crusts, Earth Planet. Sci. Lett. 141 (1996) 213–226.

[13] N. Kumar, R.F. Anderson, R.A. Mortlock, P.N. Froehlich, P.W. Kubik, B. Dittrich-Hannen, M. Suter, Increased biological productivity and export production in the glacial Southern Ocean, Nature 362 (1993) 45–48.

[14] M. Frank, Reconstruction of late Quaternary environmental conditions applying the natural radionuclides $^{230}$Th$_{ex}$, $^{10}$Be, $^{231}$Pa and $^{238}$U: A study of deep-sea sediments from the eastern Atlantic sector of the Antarctic Circumpolar Current system, Rep. Polar Res. 186 (1996) 136 pp.

[15] J. Imbrie, J.D. Hays, D.G. Martinson, A. McIntyre, A.C. Mix, J.J. Morley, N.G. Pisias, W.L. Prell, N.J. Shackleton, The orbital theory of Pleistocene climate: support from a revised chronology of the marine $\delta^{18}$O record, in: A.L. Berger, J. Imbrie, J. Hays, G. Kukla, B. Saltzman (Eds.), Milankovitch and Climate, vol. 1, Reidel, Dordrecht, 1984, pp. 269–305.

[16] A. Mangini, A. Eisenhauer, P. Walter, Response of Mn in the ocean to the climatic cycles in the Quaternary, Paleoceanography 5 (1990) 811–821.

[17] C.G. Constable, L. Tauxe, R.L. Parker, Analysis of 11 Myr of Geomagnetic Intensity variation, J. Geophys. Res. 103 (1998) 17735–17748.

[18] B. Lehman, C. Laj, C. Kissel, A. Mazaud, M. Paterne, L. Labeyrie, Relative changes of the geomagnetic field intensity during the last 280 kyears from piston cores in the Açores area, Phys. Earth Planet. Inter. 93 (1996) 269–284.

[19] P. Hartl, L. Tauxe, A precursor to the Matuyama/Brunhes transition-field instability as recorded in pelagic sediments, Earth Planet. Sci. Lett. 138 (1996) 121–135.

[20] Y.S. Kok, L. Tauxe, Saw-toothed pattern of sedimentary paleointensity records explained by cumulative viscous remanence, Earth Planet. Sci. Lett. 144 (1996) 9–14.

[21] J. Brassart, E. Tric, J.-P. Valet, E. Herrero-Bervera, Absolute paleointensity between 60 and 400 ka from the Kohala Mountain (Hawaii), Earth Planet. Sci. Lett. 148 (1997) 141–156.

[22] P.P. Kruiver, Y.S. Kok, M.J. Dekkers, C.G. Langereis, C. Laj, A pseudo-Thellier relative paleointensity record, rock magnetic and geochemical parameters in relation to climate during the last 276 kyr in the Azores region, Geophys. J. Int. in press.

[23] L. Tauxe, T. Pick, Y.S. Kok, Relative paleointensity in sediments; a pseudo-Thellier approach, Geophys. Res. Lett. 22 (1995) 2885–2888.

[24] J.H.F. Jansen, C. Alderliesten, A.J. van Bennekom, K. van der Borg, A.F.M. de Jong, Terrigenous supply of $^{10}$Be and dating with $^{14}$C and $^{10}$Be in sediments of the Angola Basin (SE Atlantic), Nucl. Instr. Meth. B 29 (1987) 311–316.

[25] M. Frank, A. Eisenhauer, W.J. Bonn, P. Walter, H. Grobe, P.W. Kubik, B. Dittrich-Hannen, A. Mangini, Sediment redistribution versus paleoproductivity change: Weddell Sea margin sediment stratigraphy and biogenic particle flux of the last 250,000 years deduced from $^{230}Th_{ex}$, $^{10}Be$ and biogenic barium profiles, Earth Planet. Sci. Lett. 136 (1995) 559–573.

[26] C. Robinson, G.M. Raisbeck, F. Yiou, B. Lehman, C. Laj, The relationship between $^{10}Be$ and geomagnetic field strength records in central North Atlantic sediments during the last 80 ka, Earth Planet. Sci. Lett. 136 (1995) 551–557.

[27] W.F. Ruddiman, A. McIntyre, Oceanic mechanisms for amplification of the 23,000-year ice-volume cycle, Science 212 (1981) 617–627.

[28] E. Bard, B. Hamelin, R.G. Fairbanks, A. Zindler, Calibration of the $^{14}C$ timescale over the past 30,000 years using mass spectrometric U/Th ages from the Barbados corals, Nature 345 (1990) 405–410.

[29] C. Laj, A. Mazaud, J.C. Duplessy, Geomagnetic intensity and $^{14}C$ abundance in the atmosphere and ocean during the past 50 kyr, Geoph. Res. Lett. 23 (1996) 2045–2048.

[30] E. Bard, Radionuclide production by cosmic rays during the last ice age, Science 277 (1997) 532–533.

[31] J.E.T. Channell, D.A. Hodell, B. Lehman, Relative geomagnetic paleointensity and $\delta^{18}O$ at ODP Site 983 (Gardar Drift, North Atlantic) since 250 ka, Earth Planet. Sci. Lett. 153 (1997) 103–118.

[32] J.E.T. Channell, D.A. Hodell, J. McManus, B. Lehman, Orbital modulation of the Earth's magnetic field intensity, Nature 394 (1998) 464–468.